Induced Growth of Asymmetric Nanocantilever Arrays on Polar Surfaces

Z. L. Wang,[1,*] X. Y. Kong,[1] and J. M. Zuo[2]

[1]*School of Materials Science and Engineering, Georgia Institute of Technology, Atlanta, Georgia 30332-0245, USA*
[2]*Department of Materials Science and Engineering, University of Illinois, Urbana-Champaign, Urbana, Illinois 61801, USA*

(Received 1 June 2003; published 30 October 2003)

We report that the Zn-terminated ZnO (0001) polar surface is chemically active and the oxygen-terminated $(000\bar{1})$ polar surface is inert in the growth of nanocantilever arrays. Longer and wider "comblike" nanocantilever arrays are grown from the (0001)-Zn surface, which is suggested to be a self-catalyzed process due to the enrichment of Zn at the growth front. The chemically inactive $(000\bar{1})$-O surface typically does not initiate any growth, but controlling experimental conditions could lead to the growth of shorter and narrower nanocantilevers from the intersections between $(000\bar{1})$-O with $\pm(01\bar{1}0)$ surfaces.

DOI: 10.1103/PhysRevLett.91.185502 PACS numbers: 61.46.+w, 81.07.–b

Ionic crystals that consist of alternating layers of oppositely charged ions, stacked parallel to the polar surfaces, produce an accumulating normal dipole moment, resulting in divergence in surface energy. The stability of the polar surfaces is one of the most interesting topics of modern surface science [1]. Crystals with polar surfaces generally have facets or exhibit massive surface reconstructions to compensate the electrostatic charge on the surface, but ZnO $\pm(0001)$ is an exception, which is stable and without reconstruction [2–4]. Structurally, the wurtzite structured ZnO crystal is described schematically as a number of alternating planes composed of fourfold tetrahedral-coordinated O^{2-} and Zn^{2+} ions, stacked alternatively along the *c* axis. The oppositely charged ions produce positively charged (0001)-Zn and negatively charged $(000\bar{1})$-O polar surfaces. Extensive theoretical and experimental studies have been carried out very recently to investigate the superior stability of the ZnO $\pm(0001)$ polar surfaces, and several mechanisms have been proposed: the decrease of the surface Zn concentration on (0001)-Zn [5]; an electronic mechanism involving the transfer of charge from oxygen to Zn [6]; and surface adsorbed atoms [7].

Here, we show that the surface polarity can induce asymmetric growth on the two opposite surfaces. Zinc oxide is a piezoelectric semiconductor material that has important applications in sensors, transducers, and actuators [8]. By introducing oxygen vacancies in ZnO, for example, its conductivity can be tuned by orders of magnitude from semiconducting to metallic [9]. Because of its unique anisotropic structure and the fastest growth along the *c* axis, the *a* or *b* axis, and the normal direction of the *a* or *b* plane, a wide range of nanostructures of ZnO have been observed [10–12]. The growth morphology is determined by both the kinetics (growth conditions) and the surface energy. In this paper, we demonstrate that the surface polarization and surface termination are important factors for determining the growth of nanocantilever arrays.

The ZnO nanostructures used in our study were synthesized by thermal evaporation of oxide powders without a catalyst. The original source material of pure zinc oxide powders was placed at the center of an alumina tube that was inserted in a horizontal tube furnace, where the temperature, pressure, and evaporation time were controlled. The tube furnace was heated to 1350 °C (the melting point of ZnO is about 1975 °C); the tube chamber pressure was kept at 300 Torr with Ar flux at about 50 sccm (standard cubic centimeter per minute). The evaporation time was 45 min at the peak temperature. During evaporation, the products were deposited onto a fused silica plate placed at the downstream end of the alumina tube, where the deposition temperature is about ~500 °C. Controlling the growth temperature is important in controlling the final growth product.

The as-synthesized sample was first analyzed by scanning electron microscopy to demonstrate the high purity, high yield, and structural control. A scanning electron microscopy (SEM) image given in Fig. 1 shows a typical

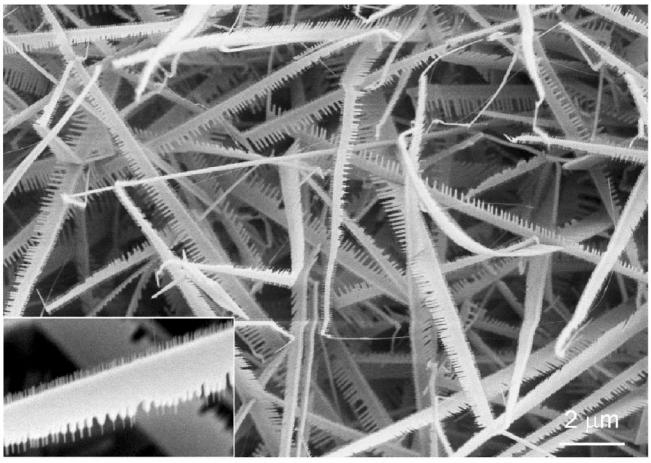

FIG. 1. Scanning electron microscopy image of the double-sided "comblike" structure grown by a solid-vapor process.

growth of comblike structure. The comb ribbon is a thin crystal slab with many parallel longer nanoteeth on one side, which are called nanotips in the discussion below, and the shorter nanoteeth on the other side are called nanofingers for easy notation [see the enlarged SEM image inset of Fig. 1 and the transmission electron microscopy (TEM) image in Fig. 2(a)].

The structure of the double-sided comb structure has been analyzed by TEM. A low magnification TEM image of the comb structure is given in Fig. 2(a), which clearly displays the double-sided teeth structure of the comb and the distribution of the nanotip arrays (longer and larger-size ones) and nanofinger arrays (shorter and narrower size ones). Electron diffraction shows that the comb ribbon grows along $[2\bar{1}\,\bar{1}\,0]$ (the *a* axis), its top/bottom surfaces are $\pm(01\bar{1}0)$, and the nanotips and nanofingers grow along $\pm[0001]$. The nanotips along [0001] have a wider base of ~300 nm and a narrow tip of width ~40 nm. It is important to point out that the nanotips growing along [0001] are rooted at the side (0001) facet. The nanofingers along $[000\bar{1}]$ are remarkably uniform in width (~ 20 nm) and length (~ 300 nm). By tilting the comb ribbon to an orientation so that it is oriented not perpendicular to the electron beam [Figs. 2(b) and 2(c)], the nanofingers growing along $[000\bar{1}]$ are found to be rooted at the edges of the ribbon, which are the intersections between the $(000\bar{1})$ and the $\pm(01\bar{1}0)$ planes [possibly the $(01\bar{1}\,\bar{1})$ and $(0\bar{1}1\bar{1})$ facets]. The white and black arrowheads in Figs. 2(b) and 2(c) indicate that the nanofingers root at the top and the bottom surfaces, respectively. This is distinctly different from the larger-size nanotips growing along [0001]. The growth front of the nanofingers is $(000\bar{1})$, side surface $\pm(2\bar{1}\,\bar{1}\,0)$, and top/bottom surfaces being $\pm(01\bar{1}0)$.

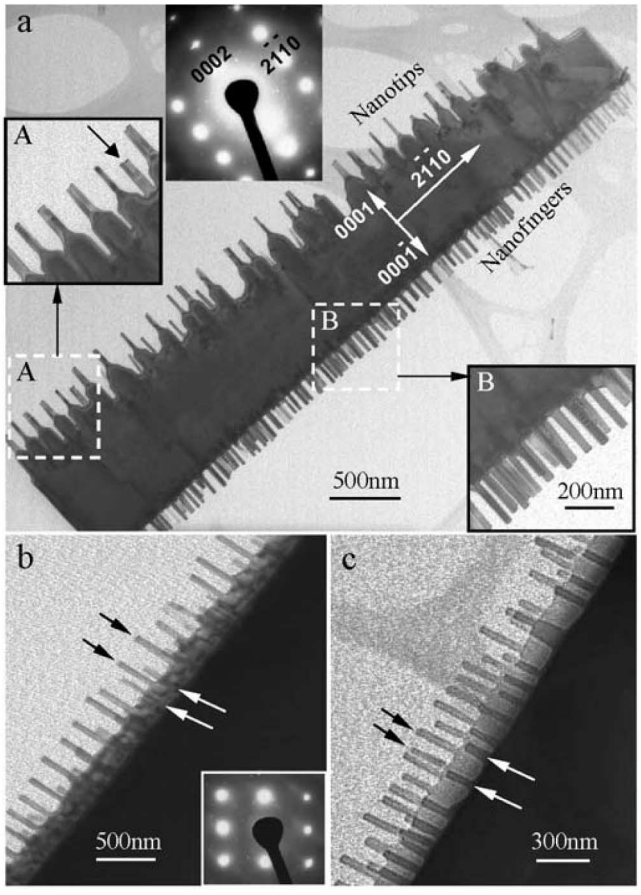

FIG. 2. (a) Transmission electron microscopy image of a double-sided comb structure, showing the distinct arrays of nanotips and nanofingers on the two sides. The inset is the corresponding electron diffraction pattern and the enlargements of two selected areas, as indicated. (b),(c) TEM images of the nanocantilever oriented at an angle with the incident electron beam so that their origin at the two edges of the main ribbon can be seen. The white and black arrowheads indicate the nanofingers rooted at the top and bottom edges, respectively.

The formation of the nanotips and nanofinger arrays on the two sides of the comb ribbon is a direct result from the surface polarity of ZnO. Figure 3(a) is a dark-field TEM image recorded from a comb structure. It is apparent that the comb ribbon has numerous dislocations, but the nanotips and nanofingers are dislocation free because of small sizes. Through the contrast presented in the dark-field TEM image, the nanotips growing along [0001] change their thickness along the growth direction, while the nanofingers along $[000\bar{1}]$ have a uniform thickness.

From the wurtzite structural model of ZnO [Fig. 3(b)], the (0001) and $(000\bar{1})$ surfaces are terminated with Zn and O, respectively, resulting in positively and negatively charged polar surfaces. To quantitatively determine the polarity of the surfaces, a convergent beam electron diffraction (CBED) pattern was recorded from the comb ribbon, as given in Fig. 3(c). The intensity distributions in the (0002) and the $(000\bar{2})$ disks are significantly different, which is due to the noncentral symmetric structure of ZnO; CBED can uniquely determine the polarity of the ZnO comb ribbon [13]. Quantitative interpretation of the CBED relies on dynamic simulations, which were performed using an improved version of the Bloch wave program [14] and the structure data from single crystal neutron diffraction [15]. A comparison of the experimental pattern with a theoretically calculated pattern is given in Figs. 3(c) and 3(d), and the excellent agreement between the two indicates that the nanotips grow out of the positively charged (0001)-Zn surface. Schematic models on the geometrical shapes and the corresponding crystallographic facets are given in Figs. 3(e) and 3(f).

To investigate the difference in nanostructure growth between the positively charged (0001)-Zn and negatively charged $(000\bar{1})$-O surfaces, high-resolution TEM was applied to image the growth fronts of the nanotips and nanofingers originated from the two surfaces, respectively. Figure 4(a) shows a $[01\bar{1}0]$ high-resolution TEM profile image recorded from the growth front of a nanotip

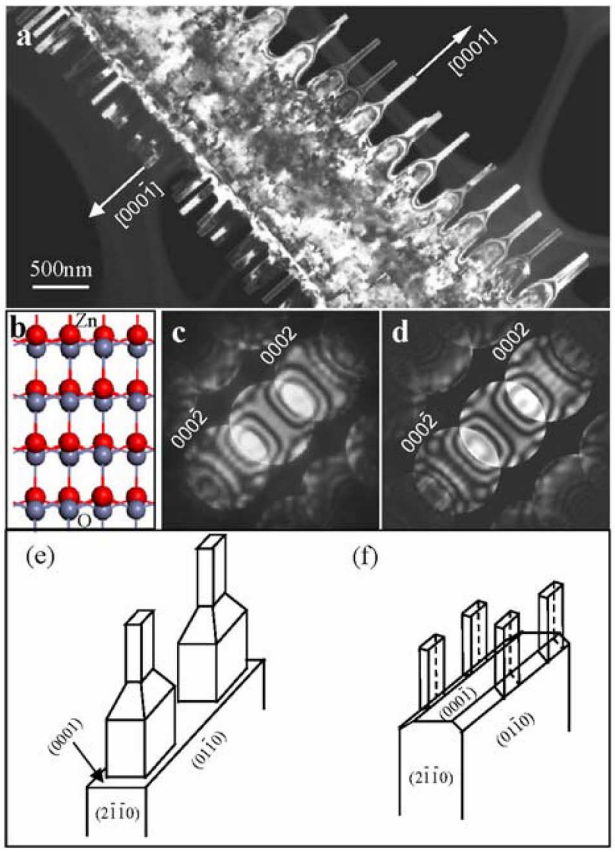

FIG. 3 (color online). (a) Dark-field TEM images recorded from the comb structure. (b) A structural model of ZnO projected along $[01\bar{1}0]$, showing polarity on the (0001) surfaces. (c) An experimental CBED pattern recorded from the ribbon. (d) A simulated CBED pattern using dynamic electron diffraction theory. The simulation includes 127 beams in both zero order and high order Laue zones, and Debye-Waller factor at room temperature. The diffraction intensities are very sensitive to thickness. The best match was found at thickness of 165 nm. $V = 200$ kV and beam direction $[01\bar{1}0]$. (e),(f) Schematic models of nanotips and nanofingers grown out of the (0001) and $(000\bar{1})$ sides, respectively.

growing along [0001]-Zn. The side and front surfaces are rough, and there are tiny nanocrystals being formed at the growth front. These nanocrystals preserve the orientation of the nanofingers and possibly grow epitaxially, and their lattice spacing fits to ZnO, as presented in the enlarged image from the growth front in Fig. 4(b). It is also noticed that the top layer of the nanocrystal has a darker contrast, possibly indicating an enrichment of Zn at the local region. A striking feature observed in the image is the presence of some dark spots at the growth front, as indicated by an arrowhead. These tiny clusters of sizes ~0.5 nm may correspond to tiny Zn clusters.

The growth front represented by $(000\bar{1})$-O shows a distinctly different structure. Figure 5 shows the high-resolution TEM image from a nanofinger growing along $[000\bar{1}]$, displaying a flat and smooth side and top surfaces.

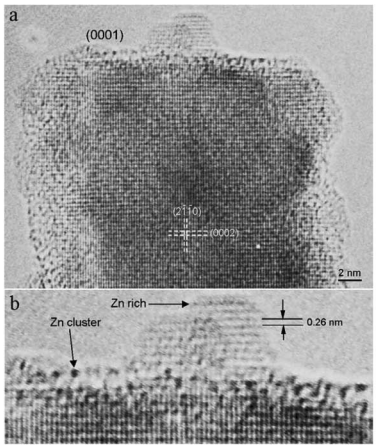

FIG. 4. (a) High-resolution TEM image recorded from a nanofinger growing along [0001], showing a rougher surface and the presence of small ZnO nanocrystals as well as possible Zn clusters at the growth front. (b) An enlargement of the growth front to display the fine structures.

The amorphous film on the surface was due to specimen handling after the growth [16]. The image clearly shows the smooth geometrical shape of the nanofingers. The inset shows an atomic resolution image of the nanofinger oriented along $[01\bar{1}0]$.

Based on the quantitative structural data presented here, the growth features observed for the comb structure with asymmetric structures on the two sides are apparently resulting from the different growth rates on the (0001)-Zn and $(000\bar{1})$-O terminated surfaces. The comb ribbon is formed by a fast growth along $[2\bar{1}\,\bar{1}\,0]$ followed

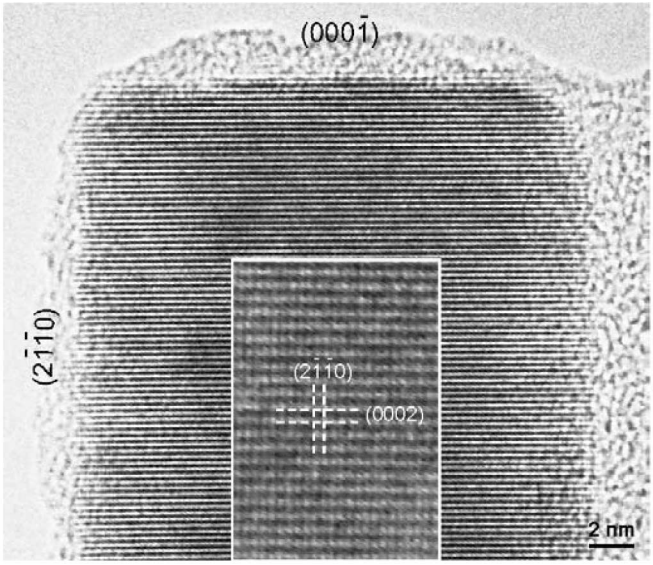

FIG. 5. High-resolution TEM image recorded from a nanocantilever growing along $[000\bar{1}]$, showing uniform and dislocation free structure. The inset is a lattice image recorded from the nanocantilever.

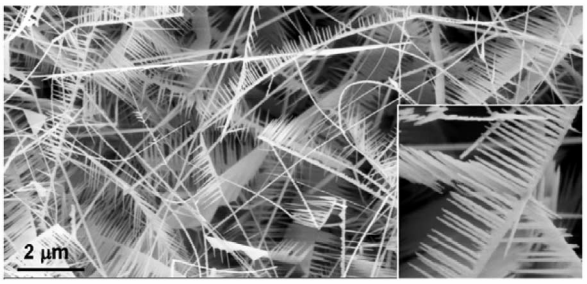

FIG. 6. SEM image of comblike structure grown by a solid-vapor process, showing nanoteeth (nanocantilevers) growing out of the [0001] side.

by a slow growth on its two sides, forming the teeth structure. This is why the nanotips and nanofingers on the two sides are uniform across the entire ribbon length. As indicated in our synthesis procedures, no catalyst was introduced in the process. The (0001)-Zn surface tends to have tiny Zn clusters at the growth front, as evidenced by the high-resolution transmission electron microscopy image given in Fig. 4. The Zn clusters as well as the local enrichment in Zn at the growth front tend to initiate the growth of ZnO analogous to the vapor-liquid-solid (VLS) growth process. Therefore, the self-catalyzed effect of the Zn clusters results in a fast growth of the nanotips. The $(000\bar{1})$-O terminated surface, however, is likely to be inert and may not exhibit an effective self-catalyzed effect; thus, the surface may not initiate the growth of nanocantilevers. From the literature, the lower energy $(01\bar{1}\,\bar{1})$ type of facets, formed at the intersection of the $(000\bar{1})$ and $(01\bar{1}0)$, could be stable for ZnO [17]. In reference to the experimental TEM images shown in Figs. 2(b) and 2(c), the growth from $(0\bar{1}1\bar{1})$ and $(01\bar{1}\,\bar{1})$ along $[000\bar{1}]$ could form arrays of nanofingers [as shown by the model in Fig. 3(f)]. This indicates that the $(000\bar{1})$ surface is inactive for initiating the teeth growth, but its edges could be active. Therefore, the nanofingers could be grown in pairs or alternate along the two one-sided edges of the comb-ribbon structure, forming arrays that may be useful for fabricating nanotweezers [18]. In practical experiments, by changing the growth kinetics so that there is no growth on the $(000\bar{1})$-O terminated surface, a comb-like structure with long teeth only on one side has been grown (Fig. 6), which was achieved by changing the local growth temperature to $\sim 600\,^{\circ}\mathrm{C}$. It is possible that a change in growth condition results in a disappearance of the $(01\bar{1}\,\bar{1})$ type of facets; thus, the chemically inert $(000\bar{1})$ surface does not initiate any teeth growth. The nanofingers shown in Fig. 6 could serve as nanocantilever arrays.

In summary, this paper demonstrates that the polarity of the ZnO (0001) surface plays an important role in determining the nanostructures grown on the surface. The self-catalyzed process is likely a mechanism for the growth of oxide nanostructures without the presence of foreign metallic catalysts. Our result shows that the surface polarity adds another important parameter in controlling the shapes of ZnO nanostructures. Because of the uniform structure and perfect geometrical shape, the nanotips and nanofingers could be potentially useful as nanocantilever arrays for nanosensors and nanotweezers.

The authors are thankful for support from NSF NIRT and NASA URIET.

*Author to whom correspondence should be addressed. Electronic address: zhong.wang@mse.gatech.edu

[1] P.W. Tasker, J. Phys. C **12**, 4977 (1979).
[2] O. Dulub, L. A. Boatner, and U. Diebold, Surf. Sci. **519**, 201 (2002).
[3] B. Meyer and D. Marx, Phys. Rev. B **67**, 035403 (2003).
[4] A. Gutierrez Sosa, T. M. Evans, S. C. Parker, C. T. Campbell, and G. Thornton, J. Phys. Chem. B **105**, 3783 (2001).
[5] O. Dulub, U. Diebold, and G. Kresse, Phys. Rev. Lett. **90**, 016102 (2003).
[6] A. Wander, F. Schedin, P. Steadman, A. Norris, R. McGrath, T. S. Turner, G. Thornton, and N. M. Harrison, Phys. Rev. Lett. **86**, 3811 (2001).
[7] V. Staemmler, K. Fink, B. Meyer, D. Marx, M. Kunat, S. Gil Girol, U. Burghaus, and Ch. Woll, Phys. Rev. Lett. **90**, 106102 (2003).
[8] S. C. Minne, S. R. Manalis, and C. F. Quate, Appl. Phys. Lett. **67**, 3918 (1995).
[9] M. Arnold, P. Avouris, Z.W. Pan, and Z. L. Wang, J. Phys. Chem. B **107**, 659 (2003).
[10] X. Y. Kong and Z. L. Wang, Nano Lett. (to be published); http://pubs3.acs.org/acs/journals/doilookup?in_-doi=10.1021/nl034463p.
[11] Y. Li, G.W. Meng, L. D. Zhang, and F. Phillipp, Appl. Phys. Lett. **76**, 2011 (2000).
[12] Z.W. Pan, Z. R. Dai, and Z. L. Wang, Science **291**, 1947 (2001).
[13] F. Vigue, P. Vennegues, S. Vezian, M. Laugt, and J.-P. Faurie, Appl. Phys. Lett. **79**, 194 (2001).
[14] J. C. H. Spence and J. M. Zuo, *Electron Microdiffraction* (Plenum, New York, 1992).
[15] T. M. Sabine and S. Hogg, Acta Crystallogr. **25**, 2254 (1969).
[16] The as-grown specimen has a clean surface but, due to contamination introduced in sample preparation for TEM observation, an amorphous carbon layer may be introduced on the surface.
[17] L. N. Demianets, D.V. Kostomarov, I. P. Kuz'mina, and S.V. Pushko, Crystallogr. Rep. (Transl. Kristallografiya) **47**, S86 (2002).
[18] P. Kim and C. M. Lieber, Science **286**, 2148 (1999).